IJPSR (2026), Volume 17, Issue 7 (Research Article)

INTERNATIONAL JOURNAL OF PHARMACEUTICAL SCIENCES AND RESEARCH

Received on 18 February 2026; received in revised form, 16 March 2026; accepted, 19 June 2026; published 01 July 2026

TRITERPENOIDS FROM *SENEGALIA ATAXACANTHA*: *IN-VITRO* ANTI-PROSTATIC CARCINOMA ACTIVITY AND *IN-SILICO* INTERACTIONS WITH ANDROGEN RECEPTORS AR:1E3G AND ARCCR:1GS4

Kennedy Ameyaw Baah [1], Desmond Nkrumah [2], Akwasi Acheampong [3], Silas Adjei [4], Linda Mensah Sarpong [1], Yakubu Jibira [5], Bismark Aboagye-Adjei [2], Isaac Kingsley Amponsah [2] and Joseph Adusei Sarkodie [*6]

Department of Science Education [1], Wesley College of Education, Kumasi, Ghana.
Department of Pharmacognosy [2], Faculty of Pharmacy and Pharmaceutical Sciences, College of Health Science, Kwame Nkrumah University of Science and Technology, Kumasi, Ghana.
Department of Chemistry [3], Faculty of Physical and Computational Sciences, College of Science, Kwame Nkrumah University of Science and Technology, Kumasi, Ghana.
Department of Herbal Medicine [4], Faculty of Pharmacy and Pharmaceutical Sciences, College of Health Science, Kwame Nkrumah University of Science and Technology, Kumasi, Ghana.
Department of Pharmacology and Toxicology [5], School of Pharmacy and Pharmaceutical Sciences, University for Development Studies, Tamale, Ghana.
Department of Pharmacognosy and Herbal Medicine [6], School of Pharmacy, University of Ghana, Legon, Accra, Ghana.

Keywords:

Senegalia ataxacantha, Triterpenoids, Prostate cancer, Cytotoxicity, Molecular docking

Correspondence to Author:
Prof. Joseph Adusei Sarkodie

Associate Professor,
Department of Pharmacognosy and Herbal Medicine, School of Pharmacy, University of Ghana, Legon, Accra, Ghana.

E-mail: jasarkodie@ug.edu.gh

ABSTRACT: Prostate cancer remains a significant global health burden, with traditional medicinal plants often used for its management, although without scientific validation. This study assessed the *in-vitro* anti-prostatic carcinoma activity of *Senegalia ataxacantha* hydroethanol extract (SA) and its triterpenoids (SA1/SA2: friedelin; SA3: friedelin/friedelinol mixture; SA4: β-sitosterol) in prostate cancer cell lines (LNCaP, VCaP, 22Rv1, PC-3, DU-145) and normal RWPE-1 cells. Cell viability was assessed following 24- and 48-hour treatments with SA (10 µg/mL), SA1–SA4 (10 µM), and abiraterone (10 µM) using the Alamar Blue assay. Molecular docking was performed using AutoDock Vina, and pharmacokinetic predictions were performed using the Protox servers.SA exhibited potent cytotoxicity, reducing LNCaP viability to 9.54 ± 5.59% and VCaP to 25.36 ± 0.52%. Friedelin showed stronger effects in VCaP (19.38 ± 0.14%) than LNCaP (73.99 ± 0.28%). The friedelin/friedelinol mixture and β-sitosterol were effective in LNCaP (38.55 ± 0.43%, 14.24 ± 0.09%) and VCaP (22.83 ± 0.16%, 25.50 ± 0.59%). In androgen-independent lines, SA reduced 22Rv1 viability to 37.63 ± 0.97%, with weaker effects in PC-3 (72.15 ± 1.06%) and DU-145 (91.00 ± 0.75%). Minimal impact on RWPE-1 (60–85% viability) indicated selectivity for cancer cells. Molecular docking revealed favourable binding to ARccr:1GS4(ΔG -6.7 to -9.4 kcal/mol), suggesting potential efficacy against castration-resistant prostate cancer (CRPC).Pharmacokinetic predictions indicated low toxicity and suitable physicochemical properties. These findings support *S. ataxacantha* and its triterpenoids as promising candidates for prostate cancer management, and merit further mechanistic, *in-vivo*, and clinical studies.

INTRODUCTION: Prostate cancer, characterised by uncontrolled proliferation of prostate cells, is a malignant neoplasm primarily affecting men over the age of 50 [1].

QUICK RESPONSE CODE

DOI: 10.13040/IJPSR.0975-8232.17(7).2054-66

This article can be accessed online on www.ijpsr.com

DOI link: https://doi.org/10.13040/IJPSR.0975-8232.17(7).2054-66

The disease progression is often slow, usually remaining asymptomatic until advanced stages, where it can invade surrounding tissues and metastasise to distant organs.

This complicates timely diagnosis and intervention, leading to several complications, including death [2]. Globally, prostate cancer is one of the most diagnosed malignancies among men. It accounted for over 1.4 million new cases and approximately 375,000 deaths in 2022, ranking as the fourth leading cause of cancer-related mortality in men

worldwide [3]. This prevalence is particularly high in sub-Saharan Africa, where limited awareness, inadequate screening programs, and constrained healthcare infrastructure contribute to late-stage presentation and poor outcomes [4].

In Ghana, prostate cancer is among the top five cancers affecting men, alongside liver cancer and non-Hodgkin lymphoma [5, 6]. Unfortunately, there has been a rising incidence, attributed to increased life expectancy, urbanisation, and evolving lifestyle patterns [7]. The true burden, however, may be underestimated due to underreporting and the absence of a comprehensive national cancer registry. Moreover, beyond its contribution to cancer-related mortality, prostate cancer imposes significant physical and emotional strain on patients and their families. This burden is compounded by the high costs of diagnosis, treatment, and long-term management, often borne out of pocket due to inadequate health insurance coverage [8, 9]. Additionally, intrinsic and acquired resistance to current anticancer drugs, spanning classical chemotherapies, targeted therapies, and emerging treatments, intensifies this scourge on affected individuals [10, 11]. Many affected families, therefore, resort to alternative and complementary treatment strategies, including medicinal plants with well-established cytotoxic effects [12, 13].

This use of plants is not solely based on financial strain and their perceived efficacy. In countries such as Ghana, cultural acceptability and preferences sometimes dictate patients' treatment choices. It has been reported that approximately 60-70% of the population employs medicinal plants for healthcare [14, 15]. Therefore, herbal medicine services have been integrated into regional and district hospitals across the country, complementing conventional healthcare. Notably, this is a step in the right direction, as several reports have documented the efficacy of plants in managing diseases, including cancer [16]. For instance, *Croton membranaceus*, a plant commonly used for prostate disorders in Ghana, demonstrated significant cytotoxicity against DLD-1 (colorectal) and MCF-7 (breast) cancer cell lines, with IC_{50} values of 16.0 and 17.4 µg/mL, respectively (17). *Zanthoxylum xanthoxyloides* showed promising cytotoxic activity against DLD-1 cells with an IC_{50} of 16.0 µg/mL(18), suggesting potential application in colorectal cancer treatment. Similarly, *Ceiba pentandra* has shown dose-dependent antiproliferative effects against HepG2 (liver) and RKO (colorectal) cancer cell lines [19]. This highlights the potential of Ghanaian medicinal plants in managing cancer and contributing to ensuring healthy lives and well-being.

That notwithstanding, several medicinal plants used folklorically to manage cancer, including prostate cancer, have not been validated scientifically. One such plant is *Senegalia ataxacantha*, highlighted in our previous work [20]. Owing to its folkloric and widespread use, it has potential as an anti-prostatic carcinoma drug, and its compounds could serve as new lead biomolecules for the synthesis and development of alternative treatment options for cancer. Thus, there is a need to investigate molecular docking techniques to provide insights into the interactions between the compounds and the target proteins implicated in prostate cancer.

Therefore, this study aimed to evaluate the anti-prostatic carcinoma activity of the hydroethanol extract of *S. ataxacantha* and its isolated triterpenoids, and to analyse the in-silico interactions of the compounds with androgen receptors AR:1e3g and ARccr:1GS4.

MATERIALS AND METHODS:

Cell Lines and Culture Conditions: Prostate cancer cell lines LNCaP (ATCC CRL-1740™), VCaP (ATCC CRL-2876™), PC-3 (ATCC CRL-1435™), DU-145 (ATCC HTB-81™), 22Rv1 (ATCC CRL-2505™), and the non-tumorigenic prostate epithelial cell line RWPE-1 (ATCC CRL-3607™) were used in this study. LNCaP cells were obtained from the American Type Culture Collection (ATCC, Manassas, VA, USA). At the same time, VCaP, PC-3, DU-145, 22Rv1, and RWPE-1 were kindly provided by Prof. Mark Rubin (Department of Biomedical Research, University of Bern, Switzerland).

LNCaP, PC-3, and 22Rv1 cells were cultured in RPMI-1640 medium (Gibco™, Thermo Fisher Scientific, Waltham, MA, USA) supplemented with 10% foetal bovine serum (FBS), 2 mM L-glutamine, 10 mM HEPES, 1 mM sodium pyruvate, and 1% penicillin-streptomycin (100 U/mL penicillin, 100 µg/mL streptomycin;

Gibco™). VCaP and DU-145 cells were maintained in Dulbecco's Modified Eagle Medium (DMEM, Gibco™) supplemented with 10% FBS, 1 mM sodium pyruvate, and 1% penicillin-streptomycin. RWPE-1 cells were cultured in keratinocyte serum-free medium (Gibco™) supplemented with 0.05 mg/mL bovine pituitary extract, 5 ng/mL human recombinant epidermal growth factor, and 1% penicillin-streptomycin. All cell lines were maintained at 37°C in a humidified 5% CO_2 atmosphere and kept below passage 30 to ensure consistency, following established protocols [21, 22].

Equipment and Materials: Cell counting was performed using a BioRad TC10™ Automated Cell Counter (506BR3656, BioRad AG, Switzerland). Experiments were conducted in sterile 96-well plates, including Sarstedt Standard R TC-96-well plates (Lot: 833925, Sarstedt AG & Co. KG, Germany) and ThermoScientific Nuclon™ Delta Surface black plates (Lot: 137101, Denmark) for fluorescence assays. Fluorescence measurements were obtained using a SpectraMax M2e microplate reader (Bucher Biotec AG, Basel, Switzerland). Analytical-grade ethanol was sourced from Fisher Scientific (Loughborough, UK), and Abiraterone acetate (Batch No: 1000818) was purchased from Sigma-Aldrich (St. Louis, MO, USA).

Extracts and Compounds from *Senegalia ataxacantha*: The study utilised hydroethanol stem bark extract (SA) and triterpenoids from *Senegalia ataxacantha* obtained in our previous study [20]. In the previous study, the stem bark was collected from Kwahu Asakraka in the Eastern region of Ghana. The plant material was authenticated by Mr Clifford Asare of the Department of Herbal Medicine, Kwame Nkrumah University of Science and Technology, and a herbarium specimen was deposited at the department's herbarium (Voucher specimen number KNUST/HM1/2020/S002). The air-dried plant material was Soxhlet-extracted with 70% hydroethanol to yield the crude extract (SA). Four (4) compounds (triterpenoids) were isolated and purified from the crude extracts through chromatographic techniques (SA1/SA2 – friedelin; SA3 - mixture of friedelin and friedelinol; SA4 - β-sitosterol). The chemical identities of the isolated compounds were characterised using spectroscopic techniques, including NMR, UV-Vis, and FTIR. The extract was stored in a desiccator, while the isolates were stored at -4 °C until required for use.

***In-vitro* Cell Viability Assay:** Human prostate cancer cell lines LNCaP, PC-3, DU-145, 22Rv1, and VCaP, together with the non-tumorigenic prostate epithelial cell line RWPE-1, were used to evaluate the cytotoxic effects of the plant extract and isolated compounds. Cells were seeded in 96-well plates (Sarstedt Standard R TC-96-well plates) at a density of 10,000 cells per well, except for VCaP cells, which were seeded at 12,000 cells per well to compensate for their relatively slower proliferation rate and to maintain assay linearity during the experiments. Cells were incubated overnight at 37°C in a humidified 5% CO_2 environment to allow adherence. The culture medium was then replaced with fresh medium containing either DMSO (0.1% v/v, control), crude extract (SA, 10 µg/mL), compounds (SA1 – SA4, 10 µM), or abiraterone (10 µM). Cells were incubated for 24 or 48 hours under the same conditions. Stock solutions of the extract, isolated compounds, and abiraterone were prepared in DMSO and subsequently diluted with culture medium to achieve the desired working concentrations. The final DMSO concentration was maintained at 0.1 % (v/v) in all wells, including the control wells, to ensure identical solvent exposure across treatment groups. Because several of the isolated triterpenoids exhibit relatively high predicted lipophilicity, this solvent system was used to ensure adequate solubilization. Visual inspection confirmed that no precipitation occurred at the working concentrations used, indicating that the compounds remained fully solubilised under assay conditions.

Cell viability was assessed using the Alamar Blue assay. Post-incubation, 10 µL of Alamar Blue (0.05 mg/mL in phosphate-buffered saline, PBS) was added to each well, and the plates were incubated in the dark at 37 °C for 4 hours. Afterwards, fluorescence was measured using a SpectraMax M2e microplate reader (Bucher Biotec AG, Basel, Switzerland) at 550 nm excitation and 590 nm emission. Cell viability was calculated as the percentage of the control [23]:

$$\% \text{ cell viability} = (rfUt - rfUb) / (rfUc - rfUb) \times 100$$

rfUt, rfUc, and rfUb depict the relative fluorescence units for the compounds/treatment, DMSO/Control, and media-only conditions, respectively. Blank wells containing culture medium and Alamar Blue reagent, but without cells, were included to account for background fluorescence. Relative fluorescence units (RFU) from blank wells were subtracted from all experimental readings before analysis.

Molecular Docking Studies of Compounds: Molecular docking was performed to investigate the binding interactions of the compounds (SA1, SA2, SA3, and SA4) with the androgen receptor (AR) ligand-binding domain. The 3D structure of the compounds was retrieved from the ZINC database [24] and converted into PDBQT format using OpenBabel.

Crystal structures of the androgen receptor ligand-binding domain were obtained from the Protein Data Bank (PDB), including AR:1E3G, representing the wild-type androgen receptor and ARccr:1GS4, representing a mutant androgen receptor associated with castration-resistant prostate cancer. Protein structures were prepared using Discovery Studio Visualizer (version 2021). Preparation involved the removal of crystallographic water molecules and heteroatoms, followed by the addition of polar hydrogens. The prepared receptor structures were then converted into PDBQT format using AutoDockTools. Metribolone (R1881), a synthetic androgen with high affinity for the androgen receptor, was used as a reference ligand because it is commonly co-crystallised with androgen receptor structures and is present in the binding pocket of the AR structure 1E3G, making it a suitable structural benchmark for docking comparisons. 9α-Fluorocortisol was also included as an additional comparator ligand [25].

Docking simulations were performed using AutoDock Vina. To explore potential ligand-binding interactions, blind docking was performed using a grid box encompassing the entire receptor. Docking calculations were performed in rigid receptor mode, and multiple binding poses were generated for each ligand. Docking outputs were processed using a custom Perl script, which extracted predicted binding free energies (ΔG), evaluated all generated binding poses for each ligand, and calculated Root Mean Square Deviation (RMSD) values to assess pose distribution and consistency. The top-ranked docking pose with the lowest predicted binding energy for each ligand was selected for further interaction analysis.

Pharmacokinetic and Toxicity Predictions: The pharmacokinetic properties of the compounds were assessed using ProTox 3.0, a web-based platform for predicting rodent oral toxicity (https://tox.charite.de/protox3/?site=faq). The tool employs predictive models based on structural similarity to compounds with established median lethal doses (LD_{50}). In addition, it identifies potential toxic fragments within the molecular structure, offering a comprehensive, integrative approach to toxicity evaluation [26]. Enzalutamide was employed as the benchmark drug in the pharmacokinetic prediction studies. *In-silico* toxicity and physicochemical properties of the compounds were predicted using ProTox-II (version 3.0), a web-based platform that estimates rodent oral toxicity and related endpoints using machine-learning models based on structural similarity to compounds with known toxicological profiles. The platform predicts parameters, including median lethal dose (LD_{50}), toxicity class, hepatotoxicity and carcinogenicity. Additionally, selected physicochemical descriptors, including LogP, topological polar surface area (TPSA), and the number of rotatable bonds, were obtained from the platform. Enzalutamide, a clinically used androgen receptor antagonist, was included as a reference compound for computational analysis.

Data Analysis: Statistical analyses were performed using GraphPad Prism (version 8.0.2, GraphPad Software, San Diego, CA, USA). Data are presented as mean ± standard deviation (SD). For each cell line and time point (24 h and 48 h), differences between treatment groups and the vehicle control were analysed using one-way analysis of variance (ANOVA) followed by Dunnett's multiple comparison test. The vehicle control (0.1 % DMSO) served as the reference group for all comparisons. Differences were considered statistically significant at $p < 0.05$.

RESULTS:

Antiprostatic Carcinoma Activity of Extracts and Compounds on Prostate Cancer Cells: The

morphological effects of SA and abiraterone on LNCaP cells were examined using phase-contrast microscopy after 24 and 48 hours of treatment **Fig. 1.** DMSO-treated control cells **Fig. 1A, B** maintained high cell density over time. SA-treated cells **Fig. 1C, D** showed a reduction in cell density at 24 hours, which was further decreased at 48 hours. Abiraterone also induced a time-dependent decrease in cell density **Fig. 1E, F.** These micrographs are presented as representative illustrations supporting the quantitative Alamar Blue viability data, rather than as independent quantitative endpoints. Cell viability assays revealed that SA and the isolated compounds exerted variable cytotoxic effects across prostate cancer cell lines, with preliminary indications of selective activity against cancer cells relative to non-tumorigenic RWPE-1 cells. In LNCaP cells, SA reduced viability to 30.03 ± 0.15% at 24 hours and 9.54 ± 5.59% at 48 hours. Among the compounds, the friedelin/friedelinol mixture (SA3) showed the greatest cytotoxicity at 24 hours (53.87 ± 0.13%), while β-sitosterol (SA4) exhibited the lowest viability at 48 hours (14.24 ± 0.09%). Friedelin (SA1) consistently showed the least cytotoxicity in LNCaP cells. Abiraterone reduced viability to a lesser extent, consistent with its mechanism as a CYP17A1 inhibitor rather than a general cytotoxic agent.

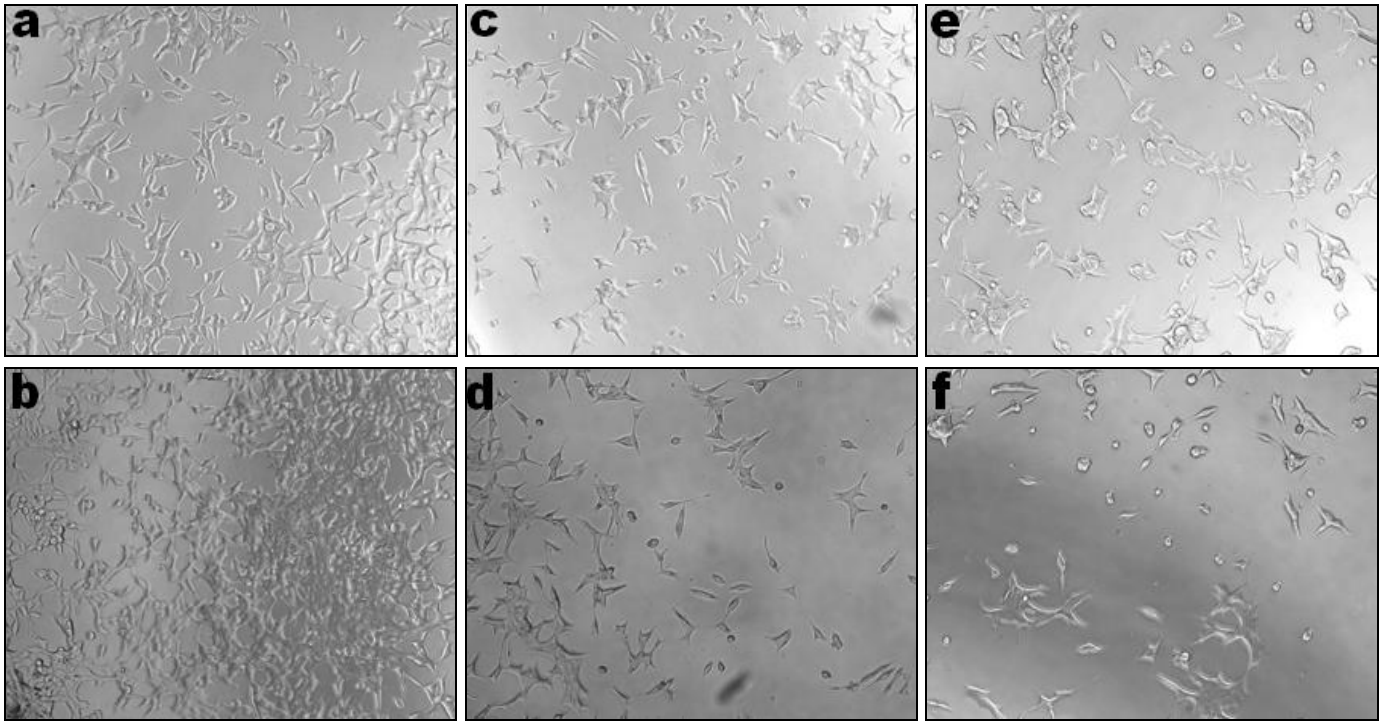

FIG. 1: REPRESENTATIVE MICROGRAPHS OF LNCAP CELLS AFTER 24 AND 48 HOURS OF TREATMENT. CELLS WERE TREATED WITH DMSO (VEHICLE CONTROL; PANELS A, B), SA CRUDE EXTRACT (PANELS C, D), OR ABIRATERONE 10 µM (PANELS E, F). PANELS A, C, AND E CORRESPOND TO THE 24-HOUR TIME POINT, WHILE PANELS B, D, AND F CORRESPOND TO THE 48-HOUR TIME POINT. IMAGES ARE PRESENTED TO ILLUSTRATE MORPHOLOGICAL CHANGES IN CELL DENSITY AND APPEARANCE THAT SUPPORT THE QUANTITATIVE VIABILITY MEASUREMENTS OBTAINED FROM THE ALAMAR BLUE ASSAY. THESE MICROGRAPHS ARE REPRESENTATIVE AND ILLUSTRATIVE AND ARE NOT INTENDED AS QUANTITATIVE ENDPOINTS.

In VCaP cells, SA was less cytotoxic (61.72 ± 0.32% at 24 hours), with the friedelin/friedelinol mixture being more active at 24 hours. By 48 hours, friedelin (SA2) displayed the greatest reduction in cell viability (14.57 ± 0.48%). In 22Rv1 cells, SA showed the highest cytotoxicity at both time points, while among the compounds, β-sitosterol was most cytotoxic at 24 hours (38.82 ± 1.63%), with friedelin emerging as the second-most cytotoxic at 48 hours. The order in decreasing cytotoxic effects on VCaP cells after 48 hrs was thus: friedelin>friedelin/fredelinol mixture>SA>β-sitosterol>abiraterone.

PC-3 cells were most affected by friedelin at 24 hours (63.29 ± 0.46%), though differences between

treatments were not statistically significant ($p > 0.05$). By 48 hours, β-sitosterol exhibited the greatest reduction in viability (61.80 ± 0.49%), followed by friedelin, SA, and the friedelin/friedelinol mixture. Abiraterone showed the weakest cytotoxic effect (89.51 ± 0.66%).

In DU-145 cells, β-sitosterol was the most cytotoxic at both 24 hours (61.28 ± 1.08%) and 48 hours (51.81 ± 0.15%), followed by the friedelin/friedelinol mixture, friedelin, and SA, which showed minimal cytotoxicity (91.00 ± 0.75%) at 48 hours. Abiraterone induced higher cytotoxicity than friedelin and SA (64.18 ± 0.26%).

RWPE-1 cells, representing non-tumorigenic prostate epithelium, were relatively resistant to SA and β-sitosterol, with viabilities of 83.43 ± 0.60% and 92.85 ± 0.21%, respectively, at 48 hours. Abiraterone was similarly non-toxic (81.72 ± 3.12%). Friedelin/friedelinol mixture (64.26 ± 0.96%) showed moderate toxicity, while friedelin was mildly cytotoxic (75.26 ± 1.09%).

TABLE 1: CYTOTOXIC EFFECT OF SA AND ABIRATERONE ON DIFFERENT PROSTATE CANCER CELLS 24 AND 48 HRS POST-TREATMENT

Extract/ compounds	LNCaP		VCaP		22Rv1		PC-3		DU-145		RWPE-1	
	Mean % cell viability											
	24 hrs	48 hrs	24 hrs	48 hrs	24 hrs	48 hrs	24 hrs	48 hrs	24 hrs	48 hrs	24 hrs	48 hrs
DMSO	100.00 ± 10.11	100.00 ± 0.12	100.00 ± 0.60	100.00 ± 0.71	100.00 ± 3.72	100.00 ± 2.18	100.00 ± 0.11	100.00 ± 0.43	100.00 ± 0.42	100.00 ± 1.07	100.00 ± 0.67	100.00 ± 3.02
SA	30.03 ± 0.15^{b}	9.54 ± 5.59^{b}	61.72 ± 0.32^{b}	25.37 ± 0.52^{b}	36.51 ± 0.80^{b}	37.63 ± 0.97^{b}	65.18 ± 0.29^{b}	72.15 ± 1.06^{b}	85.49 ± 1.52^{b}	91.00 ± 0.75^{b}	84.64 ± 3.98^{b}	83.43 ± 0.60^{b}
SA1	67.89 ± 0.42^{b}	73.99 ± 0.28^{b}	66.58 ± 1.50^{b}	19.38 ± 0.14^{b}	42.61 ± 2.43^{b}	39.13 ± 0.31^{b}	63.29 ± 0.46^{b}	66.51 ± 1.97^{b}	89.93 ± 0.12^{b}	81.90 ± 1.20^{b}	89.44 ± 4.78^{b}	85.41 ± 1.19^{b}
SA2	58.83 ± 0.24^{b}	78.18 ± 0.93^{b}	84.27 ± 0.99^{b}	14.57 ± 0.48^{b}	49.73 ± 1.62^{b}	46.15 ± 1.07^{b}	66.16 ± 0.87^{b}	77.56 ± 0.14^{b}	80.26 ± 0.15^{b}	73.59 ± 0.65^{b}	87.14 ± 5.31	75.26 ± 1.09^{b}
SA3	53.87 ± 0.13^{b}	38.55 ± 0.43^{b}	54.10 ± 1.89^{b}	22.83 ± 0.16^{b}	62.55 ± 6.73^{b}	63.31 ± 3.35^{b}	66.39 ± 0.73^{b}	79.86 ± 0.41^{b}	79.45 ± 0.88^{b}	57.53 ± 0.15^{b}	74.08 ± 0.33^{b}	64.26 ± 0.96^{b}
SA4	90.15 ± 2.19^{b}	14.24 ± 0.09^{b}	79.35 ± 0.34^{b}	25.50 ± 0.59^{b}	38.82 ± 1.63^{b}	56.15 ± 0.08^{b}	63.90 ± 0.26^{b}	61.80 ± 0.49^{b}	61.28 ± 1.08^{b}	51.81 ± 0.15^{b}	97.87 ± 2.35^{ns}	92.85 ± 0.21^{b}
Abiraterone	42.27 ± 0.20^{b}	32.28 ± 0.17^{b}	42.77 ± 1.40^{b}	30.66 ± 0.28^{b}	70.94 ± 0.49^{b}	78.93 ± 0.66^{b}	82.86 ± 0.25^{b}	89.51 ± 0.66^{b}	70.20 ± 0.51^{b}	64.18 ± 0.26^{b}	90.42 ± 3.82^{a}	81.72 ± 3.12^{b}

Data are expressed as Mean % Viability ± SD (n = 3). Statistical analysis was performed using one-way ANOVA followed by Dunnett's post hoc test, comparing each treatment group to the DMSO control. Significance is indicated as: ^{ns} Not significant ($p \geq 0.05$), ^{a} $p < 0.001$, and ^{b} $p < 0.0001$.

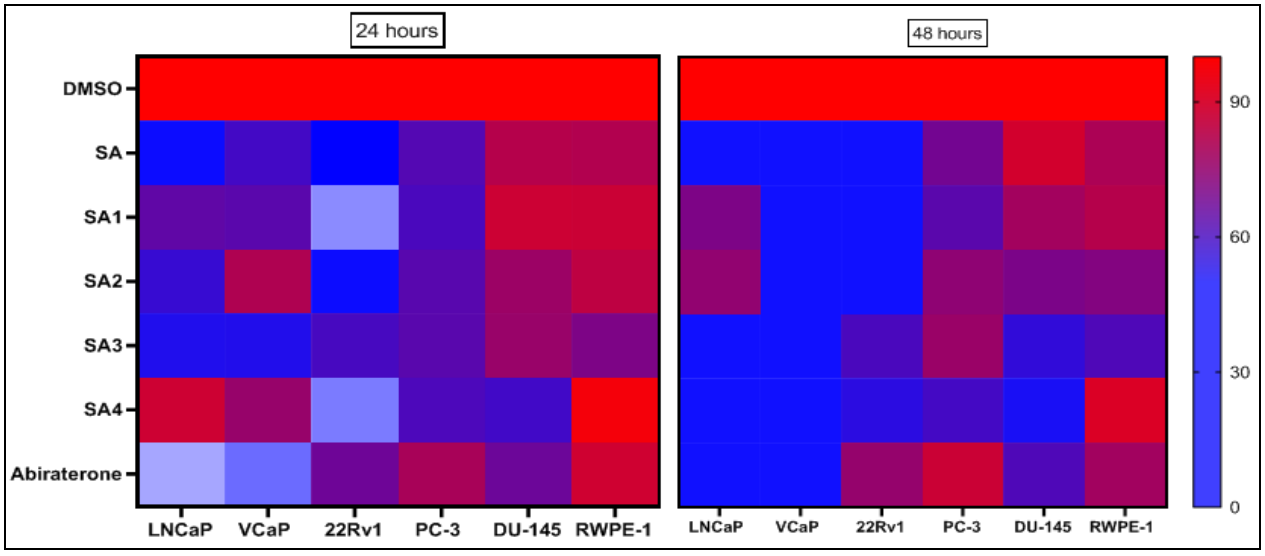

FIG. 2: HEAT MAP SHOWING THE CYTOTOXIC EFFECTS OF SA, COMPOUNDS, AND ABIRATERONE ON PROSTATE CANCER CELL LINES AT 24 AND 48 H. Values represent mean percentage cell viability relative to DMSO control (n = 3). Colour intensity represents mean percentage cell viability, with blue indicating low viability (high cytotoxicity, <30%) and red indicating high viability (low cytotoxicity, >90%). SA - *Senegalia ataxacantha* crude extract; SA1/SA2 – friedelin; SA3 – friedelin/friedelinol mixture; SA4 – β – sitosterol.

Molecular Docking against Androgen Receptors: The docking results obtained through AutoDock Vina **Table 2** reveal distinct binding affinities and interaction profiles for the compounds when interacting with the androgen receptor (AR:1E3G; **Fig. 1** and its mutant form (ARccr:1GS4; **Fig. 2**. These results provide valuable structural insights into ligand-receptor interactions but, on their own, do not confirm antiandrogenic activity and must be interpreted with caution.

Friedelin exhibits hydrophobic interactions with residues LEU 881 and HIS 885 in AR:1E3G, binding with a ΔG of -7.7 kcal/mol for the wild-type receptor and -9.4 kcal/mol for ARccr. The stronger interaction with the mutant receptor (ARccr) suggests potential relevance in targeting androgen receptor variants, though this does not confirm biological efficacy in cellular systems.

Friedelinol shows interactions with LYS 912, TYR 915, and THR 918, with binding free energies of -7.7 kcal/mol and -8.2 kcal/mol for the AR and ARccr, respectively. These moderate binding affinities indicate potential interactions, but, as with all docking results, further experimental validation is needed to confirm functional activity.

β-Sitosterol engages hydrophobically with GLU 678, VAL 684, and TRP 751, yielding a ΔG of -6.7 kcal/mol for AR:1E3G and -9 kcal/mol for ARccr. These values suggest moderate binding, with a stronger interaction observed with the mutant receptor, though this must be interpreted in the context of cellular activity, as docking scores do not necessarily correlate with biological efficacy. Metribolone demonstrates hydrophobic interactions with LEU 701, LEU 704, and MET 745, in addition to hydrogen bonding with GLN 711 and ARG 752. It exhibits ΔG values of -6.7 kcal/mol for AR and -9.3 kcal/mol for ARccr, indicating a stronger binding to the mutant receptor. While Metribolone is a known androgen receptor agonist and a reference compound in this study, its docking scores alone should not be taken as proof of antiandrogenic activity. 9α-Fluorocortisol, for which interaction data are incomplete for the wild-type AR, displays hydrophobic contacts with LEU 704, TRP 741, and MET 745 in ARccr. With the most favorable binding free energy (ΔG = -9.8 kcal/mol), it shows the strongest affinity for the mutant receptor. However, these results should be considered preliminary, as docking alone cannot confirm pharmacological activity.

TABLE 2: INTERACTION RESIDUES OF COMPOUNDS TO PROTEIN TARGETS IN THE DOCKING STUDIES

Compound	AR:1E3G Hydrophobic Interactions	AR:1E3G H-Bonds/Halogen Bonds (distance Å)	Binding free energy ΔG (kcal/mol)	ARccr:1GS4 Hydrophobic Interactions	ARccr:1GS4 H-Bonds/Halogen Bonds (distance Å)	Binding free energy ΔG (kcal/mol)
Friedelin	LEU 881, ALA 896, HIS 885	–	–7.7	PRO 682, GLN 711, ALA 748, ARG 752	–	–9.4
Friedelinol	LYS 912, TYR 915, THR 918	–	–7.7	GLU 678, GLU 681, VAL 684, PRO 801, PHE 804, LEU 805	–	–8.2
β-sitosterol	GLU 678, GLU 681, VAL 684, TRP 751, ARG 752, TYR 763, PRO 801, PHE 804, LEU 805	TYR 763 (H-bond, ~2.8 Å)	–6.7	GLU 681, VAL 715, TRP 718, LEU 744, ALA 748, ARG 752, LYS 808	–	–9.0
Metribolone	LEU 701, LEU 704, LEU 707, MET 745, MET 749, PHE 764, PHE 876	GLN 711 (H-bond, ~2.9 Å), ARG 752 (H-bond, ~3.0 Å), THR 877 (H-bond, ~2.7 Å)	–6.7	HIS 701, LEU 704, LEU 707, TRP 741, MET 745, VAL 746, PHE 764, LEU 873, ALA 877	ASN 705 (H-bond, ~2.8 Å)	–9.3
9α-fluorocortisol	LEU 704, LEU 707, TRP 741, MET 745, VAL	HIS 701 (H-bond, ~3.0 Å), ASN 705 (H-	–9.0	LEU 704, LEU 707, TRP 741, MET 745, VAL	HIS 701 (H-bond, ~3.0 Å), ASN 705 (H-bond,	–9.8

	746, PHE 764, PHE 876, ALA 877	bond, ~2.9 Å), GLN 711 (H-bond, ~2.7 Å), ARG 752 (H-bond, ~3.0 Å)		746, PHE 876, ALA 877	~2.9 Å), GLN 711 (H-bond, ~2.7 Å), ARG 752 (H-bond, ~3.0 Å)

Pharmacokinetic and Toxicity Predictions: The pharmacokinetic and toxicity profiles of the compounds were evaluated using the ProTox 3.0 platform, which predicts potential toxicity, physicochemical properties, and structural similarity to known toxic compounds. The molecular weights of the compounds ranged from 284.39 g/mol (Metribolone) to 464.44 g/mol (Enzalutamide), and their molecular refractivity values ranged from 84.71 (Metribolone) to 135.36 (Friedelinol), suggesting differences in size and polarizability that may influence membrane permeability.

Topological polar surface area (TPSA) values ranged from 17.07 (Friedelin) to 108.53 (Enzalutamide), indicating varying degrees of predicted polarity and potential cellular uptake. Lipophilicity trends, as estimated by LogP, were higher for Friedelin (8.46) and Friedelinol (8.25) relative to Enzalutamide (4.51) and Metribolone (3.72), reflecting potential differences in solubility and membrane partitioning. The predicted median lethal doses (LD_{50}) ranged from 500 mg/kg (Friedelin) to 4000 mg/kg (Metribolone), corresponding predominantly to toxicity class 4, while Metribolone was classified as class 5, suggesting moderate acute toxicity across the compounds. Prediction accuracy was generally high, though Enzalutamide (67.38%) and Metribolone (69.26%) showed slightly lower confidence. Structural similarity analysis indicated that Friedelin, Friedelinol, and Lupoel had 100% similarity to known toxic compounds, whereas Enzalutamide and Metribolone were less similar (55.91% and 76.72%, respectively), reflecting variability in potential toxicity profiles **Table 3.** Target-based toxicity predictions from ProTox indicate probabilities of inactivity or activity across several endpoints, including neurotoxicity, nephrotoxicity, and carcinogenicity **Table 4**. For example, Friedelin, Friedelinol, and β-sitosterol were predicted to be inactive for most toxicity endpoints with high probabilities (0.87–0.91), whereas Enzalutamide and Metribolone showed moderate probabilities of activity (0.62 and 0.77, respectively). Neurotoxicity was predicted to be inactive only for Friedelinol, whereas the other compounds showed varying probabilities. Nephrotoxicity predictions were generally inactive, with the highest probability for Metribolone (0.97), and carcinogenicity was largely inactive across compounds, though Metribolone displayed a lower probability (0.68). Predictions of blood-brain barrier (BBB) penetration suggested that most compounds, including Friedelin (0.99) and Metribolone (0.98), may cross the BBB.

It is important to emphasise that these predictions are computational and do not confirm pharmacological activity or mechanistic effects. For example, predicted "activity" against the androgen receptor or cytochrome P450 enzymes reflects structural likelihoods rather than experimental agonism or antagonism. While some compounds, such as Beta-sitosterol, Friedelinol, and Metribolone, showed potential interactions with CYP2C9, these results should be interpreted cautiously, as they indicate possible metabolic interactions rather than confirmed enzymatic inhibition. These computational predictions provide preliminary insights into physicochemical and toxicity profiles, but further experimental pharmacokinetic and toxicological studies are required to validate our findings.

TABLE 3: PHYSICOCHEMICAL PREDICTIONS OF COMPOUNDS FROM *IN-SILICO* STUDIES

Compound	Molecular weight	Molecular refractivity	Number of H-bond acceptors	Number of H-bond donors	Number of rotatable bonds	Topological Polar Surface area	Octanol/water partition coefficient (logP)	Predicted LD_{50}	Predicted toxicity class	Prediction accuracy	Average similarity
Friedelin	426.72	133.23	1	0	0	17.07	8.46	500	4	70.97	89.38
Friedelinol	428.73	118.45	1	1	0	20.23	8.25	940	4	67.38	55.91
β-sitosterol	414.71	134.39	1	1	6	20.33	8.02	890	4	100	100
Metribolone	284.39	135.36	2	1	0	37.3	3.72	4000	5	100	100
Enzalutamide	464.44	135.14	7	1	5	108.53	4.51	625	4	100	100

TABLE 4: PROTOX PREDICTED TOXICITY OF COMPOUNDS

			Beta-sitosterol		Enzalutamide		Friedelin		Friedelinol		Metribolone
Target	**Prediction**	**Probability**	**Prediction**	**Probability**	**Prediction**	**Probability**	**Prediction**	**Probability**	**Prediction**	**Probability**
Hepatotoxicity	Inactive	0.87	Active	0.62	Inactive	0.75	Inactive	0.78	Active	0.77
Neurotoxicity	Active	0.54	Active	0.62	Active	0.54	Inactive	0.53	Active	0.79
Nephrotoxicity	Inactive	0.89	Inactive	0.66	Inactive	0.91	Inactive	0.88	Inactive	0.97
Cardiotoxicity	Inactive	0.85	Inactive	0.89	Inactive	0.86	Inactive	0.77	Inactive	0.87
Carcinogenicity	Inactive	0.60	Inactive	0.61	Inactive	0.71	Inactive	0.79	Inactive	0.68
Cytotoxicity	Inactive	0.94	Inactive	0.75	Inactive	0.66	Inactive	0.93	Inactive	0.85
BBB-barrier	Active	0.91	Active	0.88	Active	0.99	Active	0.94	Active	0.98
Androgen Receptor (AR)	Inactive	0.83	Inactive	0.96	Inactive	0.93	Inactive	0.88	Active	1
Cytochrome CYP1A2	Inactive	0.99	Inactive	0.72	Inactive	0.93	Inactive	0.86	Inactive	0.99
Cytochrome CYP2C19	Inactive	0.98	Inactive	0.70	Inactive	0.78	Inactive	0.70	Inactive	0.69
Cytochrome CYP2C9	Active	0.64	Inactive	0.50	Inactive	0.51	Active	0.7	Active	0.79
Cytochrome CYP2D6	Inactive	0.9	Inactive	0.75	Inactive	0.90	Inactive	0.91	Inactive	0.93
Cytochrome CYP3A4	Inactive	0.99	Inactive	0.66	Inactive	0.98	Inactive	0.94	Inactive	0.85
Cytochrome CYP2E1	Inactive	1	Inactive	0.99	Inactive	0.99	Inactive	0.99	Inactive	1

DISCUSSION: The present study builds upon our previous work [20], in which triterpenoids, including friedelin (SA1/SA2), a friedelin/friedelinol mixture, and β-sitosterol, were isolated from the stem bark of *Senegalia ataxacantha*. Motivated by folkloric reports of the plant's anticancer properties, we evaluated the antiproliferative effects of the crude extract and isolated compounds on multiple prostate cancer cell lines and explored potential interactions with androgen receptors (AR) through molecular docking.

Our results demonstrated that the crude extract (SA) exhibited robust cytotoxicity against the androgen-sensitive LNCaP cells, corroborated by phase-contrast micrographs showing marked reductions in cell density **Fig. 1, Table 1.** The VCaP cell line, an androgen-sensitive, AR-amplified model representing castration-resistant prostate cancer (CRPC) with TMPRSS2-ERG fusion and AR-V7 expression [27, 28], also showed significant susceptibility to SA ($p < 0.0001$). Friedelin's enhanced activity in VCaP compared with other cell lines suggested a possible potentiation by AR-mediated signaling or VCaP-specific molecular features. This is the first report of cytotoxicity of SA, friedelin, and β-sitosterol in VCaP cells.

The extract displayed reduced, though still significant, cytotoxicity in androgen-independent models (22Rv1, PC-3, and DU-145), consistent with a partial reliance on AR-mediated mechanisms and suggesting the potential involvement of AR-independent pathways. Among these lines, 22Rv1, a clinically relevant CRPC model expressing AR splice variants [29], was more sensitive to SA than PC-3 or DU-145 cells, highlighting its potential for targeting drug-resistant prostate cancers. The cytotoxic effects of SA in PC-3 cells are reported here for the first time.

Friedelin exhibited pronounced cytotoxicity in 22Rv1 cells, comparable to SA, while being less effective in PC-3 and DU-145 cells. These findings align with Joshi *et al.* [30], who proposed CYP17A1 inhibition as a possible mechanism. The friedelin/friedelinol mixture showed moderate activity across most lines, while 3β-friedelinol demonstrated significant activity, particularly in VCaP cells, marking its first report of antiprostatic carcinoma potential. β-Sitosterol exhibited its strongest effects in LNCaP cells, followed by 22Rv1, PC-3, and DU-145, suggesting partial dependence on AR signalling and likely contribution from AR-independent mechanisms [31–35]. These results are consistent with prior studies demonstrating β-sitosterol's anticancer effects through growth inhibition, apoptosis induction, and activation of the sphingomyelin-ceramide pathway [33, 36–38].

Importantly, the non-tumorigenic RWPE-1 cells were minimally affected by SA and its compounds (cell viability >80% for SA and β-sitosterol), suggesting preferential targeting of cancer cells and reinforcing their therapeutic potential. The friedelin/friedelinol mixture showed modest

cytotoxicity in RWPE-1 cells, indicating the need for careful evaluation of selectivity in future studies. Molecular docking analyses provided a structural context for the observed cytotoxicity. Friedelin exhibited binding free energies of –7.7 kcal/mol for AR:1E3G and –9.4 kcal/mol for ARccr:1GS4, indicating enhanced binding to the mutant receptor, with hydrophobic contacts involving PRO 682, GLN 711, ALA 748, and ARG 752 **Table 2**. Friedelinol (SA3) showed ΔG values of –7.7 kcal/mol and –8.2 kcal/mol for AR:1E3G and ARccr:1GS4, respectively, interacting with residues GLU 678, GLU 681, VAL 684, PRO 801, PHE 804, and LEU 805. β-Sitosterol demonstrated moderate binding affinity (ΔG = –6.7 kcal/mol for AR:1E3G and –9.0 kcal/mol for ARccr:1GS4), forming hydrophobic interactions at GLU 681, VAL 715, TRP 718, LEU 744, ALA 748, ARG 752, and LYS 808, supplemented by a hydrogen bond with TYR 763 in the wild-type receptor. These data suggested potential efficacy against CRPC models, such as VCaP and 22Rv1, in which AR variants drive therapy resistance [30, 39]. While docking results provided mechanistic insight, we emphasise that these are computational predictions and cannot confirm AR antagonism or agonism without experimental validation.

Pharmacokinetic and toxicity predictions further supported the potential of these triterpenoids. Compounds exhibited favourable physicochemical properties, with molecular weights of 414.71–428.73 Da and logP values of 8.02–8.46, indicative of good lipophilicity, potentially enhancing cellular uptake. Predicted LD_{50} values (500–940 mg/kg) place the compounds in class 4, low-to-moderate toxicity, comparable to enzalutamide (625 mg/kg), suggesting a favourable safety profile **Table 3**. In silico toxicity predictions **Table 4** indicated inactivity in hepatotoxicity, nephrotoxicity, cardiotoxicity, carcinogenicity, and cytotoxicity for most compounds (probabilities ≥0.66). Certain compounds, including β-sitosterol and friedelinol, showed potential CYP2C9 interactions (probabilities 0.64–0.70), highlighting the need to assess possible drug-drug interactions in future studies [40]. Predicted blood-brain barrier penetration (probabilities ≥0.88) suggest broad bioavailability, but this requires *in-vivo* confirmation. Importantly, androgen receptor "activity" predictions are interpreted cautiously as computational estimations rather than mechanistic evidence of pharmacological agonism or antagonism, consistent with reviewer guidance.

This study has some limitations that should be considered when interpreting the findings. First, the biological evaluation was conducted using single screening concentrations of the crude extract and isolated compounds. While this approach enabled comparative assessment across multiple prostate cancer cell models, it did not allow determination of dose-response relationships or calculation of IC_{50} values. Consequently, selectivity indices between cancerous and non-tumorigenic cells could not be formally established. Future studies should therefore incorporate expanded concentration ranges to generate dose-response curves and more quantitative potency metrics. Second, although the Alamar Blue assay provides a reliable measure of cellular metabolic activity and viability, additional mechanistic studies such as apoptosis assays, cell cycle analysis, or androgen receptor reporter assays would be necessary to further elucidate the molecular mechanisms underlying the observed antiproliferative effects.

Third, the molecular docking analyses presented here represent computational predictions of ligand-receptor interactions that provide valuable structural insights but do not confirm biological activity within cellular systems. Similarly, toxicity and physicochemical properties were assessed using *in-silico* prediction tools, and experimental pharmacokinetic and toxicological studies will be required to validate these predictions. In addition, abiraterone was selected as the comparator because it is a clinically established inhibitor of CYP17A1-mediated androgen biosynthesis and is widely used in the treatment of advanced prostate cancer, particularly castration-resistant prostate cancer. In this study, abiraterone served as a functional comparator for androgen-axis-targeted inhibition, allowing evaluation of whether the extract and isolated compounds produced effects comparable to a clinically relevant endocrine-targeting therapy. However, it should be noted that abiraterone is not a general cytotoxic agent and may be less relevant in androgen-independent cell lines. The use of a single comparator, therefore, represents an additional limitation of the present study and should be addressed in future work by including

complementary reference agents. Despite these limitations, the study provides preliminary evidence suggesting that the investigated triterpenoids warrant further investigation as potentially lead compounds in prostate cancer research.

CONCLUSION: The hydroethanol extract and the triterpenoids isolated from *Senegalia ataxacantha* exhibited selective cytotoxicity against prostate cancer cell lines, while sparing normal RWPE-1 epithelial cells. SA and its components exerted the strongest effects, indicating that their activity may involve both androgen receptor-dependent and independent mechanisms. Molecular docking suggested that these compounds can interact with the androgen receptor, including CRPC-relevant mutant forms, providing a structural rationale for their potential efficacy against therapy-resistant prostate cancer. *In-silico* pharmacokinetic and toxicity assessments indicated favourable lipophilicity, moderate predicted safety, and low likelihood of off-target effects, though these findings require experimental confirmation.

These results provided scientific support for the traditional use of *S. ataxacantha* in managing prostate disorders and identified its triterpenoids as promising leads for further anticancer drug development. Follow-up studies should focus on dose-response profiling, mechanistic validation, and *in-vivo* efficacy and safety testing to establish their true therapeutic potential.

ACKNOWLEDGEMENTS: The authors are indebted to the technical staff of the Departments of Chemistry, Pharmacognosy, and Herbal Medicine at Kwame Nkrumah University of Science and Technology for their invaluable assistance. We are also indebted to Prof. Amit Pandey's Lab at the University of Bern (Switzerland) for making their lab available for *in-vitro* and molecular docking studies.

Author Contributions: Kennedy Ameyaw Baah: Methodology, Writing – review & editing, Writing – original draft. Desmond Nkrumah: Writing – review & editing, Data curation. Akwasi Acheampong: Supervision, Writing – review & editing, Conceptualization. Silas Adjei: Methodology, Formal analysis, Data curation, Conceptualization. Linda Mensah Sarpong: Methodology, Writing – review & editing, Writing – original draft, Formal analysis, Data curation, Conceptualization. Jibira Yakubu: Writing – review & editing, Writing – original draft, Formal analysis. Bismark Aboagye-Adjei: Methodology, Formal analysis, Data curation, Conceptualization. Isaac Kingsley Amponsah: Methodology, Writing – review & editing, Writing – original draft, Formal analysis, Conceptualization. Joseph Adusei Sarkodie: Data curation, Writing – review & editing, corresponding author.

Funding: This research received no external funding or any specific grant from funding agencies in the public, commercial, or not-for-profit sectors.

Data Availability: All datasets used and/or analysed during the current study are available in the manuscript and could also be requested from the corresponding author.

Ethical Approval: Ethical Approval is not applicable for this article.

CONFLICTS OF INTEREST: The authors declare that they have no known competing financial interests or personal relationships that could have influenced the work reported in this paper.

REFERENCES:

1. Groeben C and Wirth MP: Prostate cancer: Basics on clinical appearance, diagnostics and treatment. Med Monatsschr Pharm 2017; 40(5): 192–201.
2. Crohns M, Westermarck T and Atroshi F: Prostate Cancer, Inflammation and Antioxidants. In: Advances in Prostate Cancer 2013.
3. Bray F, Laversanne M, Sung H, Ferlay J, Siegel RL and Soerjomataram I: Global cancer statistics 2022: GLOBOCAN estimates of incidence and mortality worldwide for 36 cancers in 185 countries. CA Cancer J Clin 2024; 74(3): 229–63.
4. Jalloh M, Cassell A, Niang L and Rebbeck T: Global viewpoints: updates on prostate cancer in Sub-Saharan Africa. Vol. 133, BJU International. John Wiley and Sons Inc 2024; 6–13.
5. Laryea DO, Awittor FK, Sonia C and Boadu KO: Three Years of Population-Based Cancer Registration in Kumasi: Providing Evidence for Population-Based Cancer Surveillance in Ghana. Online J Public Health Inform 2016; 8(1).
6. Laryea DO, Awuah B, Amoako YA, Osei-Bonsu E, Dogbe J and Larsen-Reindorf R: Cancer incidence in Ghana, 2012: Evidence from a population-based cancer registry. BMC Cancer 2014; 14(1).

7. Jemal A, Center MM, DeSantis C and Ward EM: Global patterns of cancer incidence and mortality rates and trends. Vol. 19, Cancer Epidemiology Biomarkers and Prevention 2010; 1893–907.
8. Blinder V and Gany FM: Financial Toxicity in Cancer Treatment. In: Psycho-Oncology. Oxford University Press 2021; 616–20.
9. PDQ Adult Treatment Editorial Board: Financial Toxicity (Financial Distress) and Cancer Treatment (PDQ®): Patient Version. PDQ Cancer Information Summaries. 2002
10. Wang X, Zhang H and Chen X: Drug resistance and combating drug resistance in cancer. Cancer Drug Resist 2019; 2(2): 141–60.
11. Ankathil R: The mechanisms and challenges of cancer chemotherapy resistance: A current overview. Eur J Mol Clin Med 2019; 6(1): 26–34.
12. Nataru S, Pulicherla Y and Gaddala B: A review on medicinal plants as a potential source for cancer. Vol. 26, International Journal of Pharmaceutical Sciences Review and Research 2014; 235–48.
13. Molassiotis A, Fernandez-Ortega P, Pud D, Ozden G, Scott JA and Panteli V: Use of complementary and alternative medicine in cancer patients: A European survey. Ann Oncol 2005; 16(4): 655–63.
14. Mintah SO, Archer MA, Asafo-Agyei T, Ayertey F, Jnr PAA and Boamah D: Medicinal Plant Use in Ghana: Advancement and Challenges. Am J Plant Sci 2022; (3): 316–58.
15. Agbovie T, Amponsah K, Crentsil OR, Dennis F, Odamtten GT and Ofosuhene-Gyan W: Conservation and Sustainable Use of Medicinal Plants in Ghana. Prep Phytopharm Manag Disord 2002; 409–27.
16. Sawadogo WR, Schumacher M, Teiten MH, Dicato M and Diederich M: Traditional West African pharmacopoeia, plants and derived compounds for cancer therapy. Biochem Pharmacol 2012; 84(10): 1225–40.
17. Ayim JA, Bayor MT, Phillips RM, Shnyder SD and Wright CW: The evaluation of selected ghanaian medicinal plants for cytotoxic activites. J Sci Technol 2008; 27(3).
18. Misra LN, Wouatsa NAV, Kumar S, Venkatesh Kumar R and Tchoumbougnang F: Antibacterial, cytotoxic activities and chemical composition of fruits of two Cameroonian *Zanthoxylum* species. J Ethnopharmacol 2013; 148(1): 74–80.
19. Addy BS, Firempong CK, Komlaga G, Addo-Fordjour P, Domfeh SA and Afolayan O: *In-vitro* antiproliferative activities of some Ghanaian medicinal plants. Clin Phytoscience 2024; 10(1).
20. Baah KA, Acheampong A, Amponsah IK, Adjei S, Jibira Y and Nketia RI: "Hydroethanol extract and triterpenoids of Senegalia ataxacantha show antiplasmodial activity and the compounds are predicted to inhibit parasite lactate dehydrogenase (pfLDH) as indicated by molecular docking studies." Sci African 2024; 26: 02455.
21. Wróbel TM, Rogova O, Sharma K, Velazquez MNR, Pandey AV and Jørgensen FS: Synthesis and Structure–Activity Relationships of Novel Non-Steroidal CYP17A1 Inhibitors as Potential Prostate Cancer Agents. Biomolecules 2022; 12(2).
22. Malikova J, Brixius-Anderko S, Udhane SS, Parween S, Dick B and Bernhardt R: CYP17A1 inhibitor abiraterone, an anti-prostate cancer drug, also inhibits the 21-hydroxylase activity of CYP21A2. J Steroid Biochem Mol Biol 2017; 174: 192–200.
23. Sharma K, Lanzilotto A, Yakubu J, Therkelsen S, Vöegel CD and Du Toit T: Effect of Essential Oil Components on the Activity of Steroidogenic Cytochrome P450. Biomolecules 2024; 14(2): 203.
24. Irwin JJ, Tang KG, Young J, Dandarchuluun C, Wong BR and Khurelbaatar M: ZINC20 - A Free Ultralarge-Scale Chemical Database for Ligand Discovery. J Chem Inf Model 2020; 60(12): 6065–73.
25. Matias PM, Carrondo MA, Coelho R, Thomaz M, Zhao XY and Wegg A: Structural basis for the glucocorticoid response in a mutant human androgen receptor (ARccr) derived from an androgen-independent prostate cancer. J Med Chem 2002; 45(7): 1439–46.
26. Drwal MN, Banerjee P, Dunkel M, Wettig MR and Preissner R: ProTox: A web server for the *in-silico* prediction of rodent oral toxicity. Nucleic Acids Res. 2014; 42(1): 53–8.
27. Korenchuk S, Lehr JE, McLean L, Lee YG, Whitney S and Vessella R: VCaP, a cell-based model system of human prostate cancer. *In-vivo* (Brooklyn) 2001; 15(2): 163–8.
28. Hermans KG, Van Marion R, Van Dekken H, Jenster G, Van Weerden WM and Trapman J: TMPRSS2:ERG fusion by translocation or interstitial deletion is highly relevant in androgen-dependent prostate cancer, but is bypassed in late-stage androgen receptor-negative prostate cancer. Cancer Res 2006; 66(22): 10658–63.
29. Dehm SM, Schmidt LJ, Heemers HV, Vessella RL and Tindall DJ: Splicing of a novel androgen receptor exon generates a constitutively active androgen receptor that mediates prostate cancer therapy resistance. Cancer Res 2008; 68(13): 5469–77.
30. Joshi BP, Bhandare VV, Vankawala M, Patel P, Patel R and Vyas B: Friedelin, a novel inhibitor of CYP17A1 in prostate cancer from Cassia tora. J Biomol Struct Dyn 2023; 41(19): 9695–720.
31. Wang H, Wang Z, Zhang Z, Liu J and Hong L: β-Sitosterol as a Promising Anticancer Agent for Chemoprevention and Chemotherapy: Mechanisms of Action and Future Prospects. Advances in Nutrition. Elsevier B.V 2023; 14: 1085–110.
32. Von Holtz RL, Fink CS and Awad AB: β-Sitosterol activates the sphingomyelin cycle and induces apoptosis in LNCaP human prostate cancer cells. Nutr Cancer 1998; 32(1): 8–12.
33. Jourdain C, Tenca G, Deguercy A, Troplin P and Poelman D: *In-vitro* effects of polyphenols from cocoa and β-sitosterol on the growth of human prostate cancer and normal cells. Eur J Cancer Prev 2006; 15(4): 353–61.
34. Awad AB, Fink CS, Williams H and Kim U: *In-vitro* and *in-vivo* (SCID mice) effects of phytosterols on the growth and dissemination of human prostate cancer PC-3 cells. Eur J Cancer Prev 2001; 10(6).
35. Scholtysek C, Krukiewicz AA, Alonso JL, Sharma KP, Sharma PC and Goldmann WH: Characterizing components of the Saw Palmetto Berry Extract (SPBE) on prostate cancer cell growth and traction. Biochem Biophys Res Commun 2009; 379(3): 795–8.
36. Awad AB, Burr AT and Fink CS: Effect of resveratrol and β-sitosterol in combination on reactive oxygen species and prostaglandin release by PC-3 cells. Prostaglandins Leukot Essent Fat Acids 2005; 72(3): 219–26.
37. Scholtysek C, Krukiewicz AA, Alonso JL, Sharma KP, Sharma PC and Goldmann WH: Characterizing components of the Saw Palmetto Berry Extract (SPBE) on prostate cancer cell growth and traction. Biochem Biophys Res Commun 2009; 379(3): 795–8.

38. Webber MM, Quader STA, Kleinman HK, Bello-DeOcampo D, Storto PD and Bice G: Human cell lines as an *in-vitro*/*in-vivo* model for prostate carcinogenesis and progression. Prostate 2001; 47(1): 1–13.
39. Li Y, Chan SC, Brand LJ, Hwang TH, Silverstein KAT and Dehm SM: Androgen receptor splice variants mediate enzalutamide resistance in castration-resistant prostate cancer cell lines. Cancer Res 2013; 73(2): 483–9.
40. Wei J, Zhang H and Zhao Q: *In-vitro* inhibitory effects of friedelin on human liver cytochrome P450 enzymes. Pharm Biol 2018; 56(1): 363–7.

How to cite this article:
Baah KA, Nkrumah D, Acheampong A, Adjei S, Sarpong LM, Jibira Y, Aboagye-Adjei B, Amponsah IK and Sarkodie JA: Triterpenoids from *Senegalia ataxacantha*: *in-vitro* anti-prostatic carcinoma activity and *in-silico* interactions with androgen receptors AR:1E3G and ARCCR:1GS4. Int J Pharm Sci & Res 2026; 17(7): 2054-66. doi: 10.13040/IJPSR.0975-8232.17(7).2054-66.